Revista Mexicana de Astronomía y Astrofísica, **39**, 127–137 (2003)

THE RADIAL VELOCITY PROFILES OF SOME PROPLYDS IN THE ORION NEBULA[1]

E. de la Fuente,[2,3] M. Rosado,[2] L. Arias,[2] and P. Ambrocio-Cruz[2]

Received 2002 June 12; accepted 2003 March 18

RESUMEN

Usamos los datos obtenidos con un interferómetro de Fabry-Perot de barrido en la parte central de la Nebulosa de Orión para estudiar los *proplyds* de esta región. Encontramos que la interferometría de Fabry-Perot es una técnica efectiva para detectar e identificar a los *proplyds*. Muchos *proplyds* y objetos candidatos se detectan sólo después de aplicar técnicas de procesamiento a los cubos de velocidades de Fabry-Perot. Adicionalmente, presentamos los perfiles de velocidad radial, sustraídos de la region H II, de la mayoría de los *proplyds* detectados (13), así como de los candidatos (3). A partir de éstos, estimamos las propiedades cinemáticas más importantes de estos objetos. Encontramos que todos los *proplyds* tienen velocidades corridas al rojo con respecto a la Nebulosa de Orión. Encontramos también que los *proplyds* que estudiamos tienen valores típicos de pérdida de masa y de escala temporal del disco y discutimos las implicaciones de esto, tomando en cuenta que nuestro estudio es sobre una buena proporción de *proplyds*. Finalmente, vemos que nuestros perfiles de velocidad sugieren que una buena fracción de *proplyds* presentan *microjets* monopolares.

ABSTRACT

We use Hα scanning Fabry-Perot interferometric data on the Orion Nebula in order to study the proplyds of the central region. We find that Fabry-Perot interferometry constitutes an effective technique for the detection and identification of proplyds. Some of the proplyds and proplyd candidates become noticeable only after data processing of the Fabry-Perot velocity cubes. In addition, we present the H II region subtracted radial velocity profiles of most of the identified proplyds (13) and proplyd candidates (3). We estimate from these profiles their main kinematic properties. We find that all of them have velocities redshifted relative to the Orion nebular emission. The studied proplyds show typical values of mass loss and disk lifetimes and we discuss the implications of these values, taking into account the fact that this study is done over a large quantity of proplyds. Finally, we find that our velocity profiles suggest that a large fraction of proplyds have monopolar microjets.

Key Words: **CIRCUMSTELLAR MATTER — H II REGIONS — ISM: INDIVIDUAL (ORION NEBULA) — ISM: KINEMATICS AND DYNAMICS — STARS: FORMATION**

1. INTRODUCTION

The proplyds (PROtoPLanetarY DiskS) are photoevaporating circumstellar disks around young stellar objects (YSOs). They are shaped during the interaction between the photoionizing flux from a hot external star and the photoevaporated flow of the disk. The photoevaporated flow passes through a D-type ionization front (IF) producing a weak shock that lies just inside the IF, generating a slight density enhancement that is seen in silhouette. The bright proplyd cusp corresponds to the photoevaporated flow from the head of the proplyd driven by the ionizing photons from the hot external star. The tails are formed by the ionized photoevaporated flow

[1] Based on observations collected at the Observatorio Astronómico Nacional, San Pedro Mártir, B. C., México.

[2] Instituto de Astronomía, Universidad Nacional Autónoma de México, México, D. F.

[3] Instituto de Astronomía y Meteorología, Depto. de Física, CUCEI, Universidad de Guadalajara, México.

driven by the diffuse UV photons radiated from the nebula. Several proplyds present a standoff shock produced when the photoevaporated flow from the proplyd cusp interacts with the stellar wind from the external hot star. Some proplyds present monopolar microjets (Meaburn et al. 1993; Bally, O'Dell, & McCaughrean 2000; Henney et al. 2002) that could be interpreted as collimated outflows from the YSO.

The term "proplyd" was coined by C. R. O'Dell to name the six nebulosities discovered for the first time by Laques & Vidal (1979) and called LV objects. The proplyds were identified as young stars with circumstellar clouds photoionized from the exterior by θ^1 Orionis C, by means of VLA observations (Garay, Moran, & Reid 1987; Churchwell et al. 1987) and from UKIRT 2.2 μm K-band images (Meaburn 1988). Bally et al. (1998a), Henney & O'Dell (1999), García-Arredondo, Henney, & Arthur (2001), and Henney et al. (2002) present a scheme for proplyd formation. These ideas are based on the photoevaporating flow models developed by Dyson (1968), Bertoldi (1989), Henney & Arthur (1998), Johnstone, Hollenbach, & Bally (1998), and Storzer & Hollenbach (1999).

The proplyds were imaged in 1993 with the *Hubble Space Telescope* (*HST*), revealing for the first time their morphology: silhouettes, bow shocks and even circumstellar disks (O'Dell, Wen, & Hu 1993; O'Dell & Wen 1994). The heads of many of them, pointing towards θ^1 Orionis C (O'Dell 1998; Bally et al. 1998a), confirm the influence of this star on proplyd emission and morphology. The proplyds have mass-loss rates of 10^{-6}–$10^{-7}\,M_\odot\,\mathrm{yr}^{-1}$ (Churchwell et al. 1987; Henney & O'Dell 1999), radial velocities of 24 to 30 km s^{-1} (Henney & O'Dell 1999), diameters of 10^{-4}–10^{-3} pc (O'Dell 1998) and disk masses of 0.005–0.002 $M_\odot$ (Johnstone et al. 1998; Bally et al. 1998b). These values are estimated from extinction measures of the silhouette disks on the background H II region emission (Throop et al. 2001) or from CO millimetric observations of the thermal dust emission from their disks (Bally et al. 1998b). These latter observations give evidence of accretion disks surrounding young stellar objects (Sargent 1996, and references therein).

The importance of studying the physics of the proplyds stems mainly from their astrophysical and astrobiological aspects. Knowing the systemic velocities and the radial velocity profiles of the proplyds we can compare the observations with the existing theoretical models in order to present arguments in favor of the existence of accretion disks in them, and to better understand the interaction of the photoevaporated material and the photoionizing flux. Also, from the determination of the velocity of the gas, in combination with observations of the surface brightness in Hα, we can derive the mass-loss rate (O'Dell 1998). Due to the fact that Orion is a nebula rich in interstellar phenomena and that it displays a gradient in the radial velocity across its area, we can, with Fabry-Perot techniques, identify the different velocity components of a radial velocity profile, in this case, the H II region velocity component and the proplyd velocity component. This work complements a previous work (Rosado et al. 2001), where a study of the kinematics of the gas, Herbig-Haro (HH) objects, and jets at large scales in the Orion Nebula, was presented. That work found blueshifted components in the HH objects, velocity gradients in the Orion Nebula (from +5 to +20 km s^{-1}), and proposed that HH 202, HH 203, and HH 204 were part of a large bipolar outflow centered near the E-W jet discovered by O'Dell et al. (1997).

Spectroscopic studies in [O III] (λ5007 Å) of the proplyds reported by Laques & Vidal (1979) were made by Meaburn (1988), Massey & Meaburn (1993, 1995), Meaburn et al. (1993), and Henney et al. (1997) using slit spectrometers. Meaburn (1988) published the first [O III] position-velocity diagrams showing that the proplyds LV 1 and LV 2 (according to Laques & Vidal's 1979 notation for proplyds) have distinctive velocities as compared with the velocity of the H II region. In these diagrams, the proplyds show redshifted velocities up to $V_{\mathrm{hel}} = +160\,\mathrm{km\,s^{-1}}$. Meaburn et al. (1993) show [O III] position-velocity diagrams where LV 2, LV 3, and LV 5 can be distinguished against the low receding velocities of the Orion Nebula. These authors also identify two high redshifted velocity objects that we will discuss in § 3.3. While these authors have shown position-velocity diagrams contaminated by the H II region emission for most of the objects, they have published, for the first time, the [O III] radial velocity profile of a proplyd (LV 2), subtracted from the H II region velocities. In Massey & Meaburn (1995), non-H II region subtracted position-velocity diagrams of proplyds LV 1, LV 2, LV 3, 170-334, and 170-337 (according to O'Dell & Wen's 1994 proplyd's notation) are shown. Keck high-resolution slit spectroscopy of proplyds at several ions including Hα, Hβ, [N II] (λ6583 Å), [O I] (λ6300 Å), [S III] (λ6312 Å), He I (λ5876 Å), [S II] (λ6731 Å), and [O III] (λ4959 Å) is presented by Henney & O'Dell (1999) for four proplyds. It is interesting to note that the specific proplyds reported in Henney & O'Dell's paper are different from the proplyds studied by Meaburn and collaborators. In addition to the previous [O III] velocity features reported by Meaburn et al., Henney & O'Dell reported velocity profiles presumably coming from the proplyd cusp. Indeed, they show ion velocity profiles without any high–redshifted velocities (the FWHMs visible in the displayed profiles are $\sim 40\,\mathrm{km\,s^{-1}}$). On the other hand, O'Dell et al. (1997) present a Fabry-Perot kinematic study at [O III] (λ5000 Å) and [S II] (λ6717 and 6731 Å) of the inner region of the Orion Nebula, discovering new high velocity features, and studying the emission of some proplyds. With these spectroscopic studies it is possible to determine the flow velocity and, from the [C III]/C III] line-ratio and/or Hα emission measure, the density of the ionization front (Bally et al. 1998a). These authors also present optical *HST* studies and ultraviolet observations of young stellar objects (YSOs), including the first UV spectra in the spectral range between 1400 and 3000 Å.

Given that planet formation can occur in the protoplanetary disks and, as a consequence, life can evolve there, the interest for astrobiological studies of proplyds stems from the fact that proplyds unveil the otherwise elusive protoplanetary disks. In this sense, proplyds are an important laboratory for determining, at high spatial resolution, several properties of the protoplanetary disks, such as masses, velocities and extensions. The proplyds are also useful for statistical studies of these issues. However, the protoplanetary disks revealed by the proplyds are subject to the strong UV flux of the exterior star that makes them visible. Thus, the photoevaporation of the protoplanetary disk of the proplyd could inhibit planet formation, or change its conditions. Recent studies (Bally et al. 1998b; Bally 2001; Throop et al. 2001) have shown that planet formation in irradiated protoplanetary disks (like proplyds) can only occur in special situations and conditions: disk mass $\geq 0.13\,M_\odot$ and dust particle radius (silicates+ices) $\geq 5\,\mu$m. In this context, Throop et al. (2001), through Hα and Paα *HST* images, obtained an extinction curve of the proplyd 114-426 and they found that a theoretical extinction curve dominated by dust grains with radii $\geq 5\,\mu$m fitted the observations well. They also present 1.3 mm OVRO observations suggesting that the dust growth reaches sizes of few mm, and they develop a numerical model to explain the behavior and evolution of dust grains in externally irradiated proplyds, including photo-destruction processes. Thus, they have shown that after 10^5 yr, small grains are entrained in the photoevaporative flow resulting in disks with maximum sizes of 40 AU. For disk masses as large as $0.2\,M_\odot$, the grain growth reaches a radius of meters at 10 AU from the YSO and 1 mm at 500 AU, in less than 10^5 yr. These sizes allow the dust to resist the photoevaporation process. By 10^6 yr, nearly all ice and gas is removed by photosputtering, inhibiting the Kuiper belt formation and leaving only the possibility of rocky planet formation. Therefore, it is possible that in the environments of star-forming regions like Orion, Jupiter-like planets are not formed in the standard way because it would require 10^6 to 10^7 yr (Ruden 1999, and references therein). Such Jovian planets could be present if they form in a timescale of 10^3 yr (Boss 1997), for disk masses $\geq 0.13\,M_\odot$. Since a large quantity of stars seems to be formed in large and dense clusters such as Orion (although there are star-forming complexes such as the Taurus where no massive stars are present), this leads to the conclusion that planet-formation models should be revised in order to include the destructive effects of the UV flux of newly formed massive stars in star-forming environments similar to Orion's. The possibilities for planetary systems to form in the Orion Nebula are described in Throop, Bally, & Esposito (2002).

2. OBSERVATIONS AND REDUCTIONS

Scanning Fabry-Perot (FP) data cubes were obtained from 1996 November 30 to December 5 with the PUMA Scanning Fabry-Perot Interferometer (Rosado et al. 1995) at the f/7.5 Cassegrain focus of the 2.1 m telescope of the Observatorio Astronómico Nacional at San Pedro Mártir B. C., México. A 1024×1024 thinned Tektronix CCD detector with an image scale of $0.59''\,\mathrm{pixel^{-1}}$, each pixel measuring $24\,\mu$m, was used only in its central 512×512 pixels, covering a field of $5'$, centered on the Trapezium stars. We have used an Hα filter and scanned the FP gap in 48 positions, giving a sampling spectral resolution of $19\,\mathrm{km\,s^{-1}}$ (see Rosado et al. 2001 for further details). The data reduction was carried out using the software CIGALE (Le Coarer et al. 1993).

3. RESULTS

3.1. *Unsharp-Masking Technique and Proplyd Identification*

We were able to identify the proplyds: 158-323 (LV 5), 158-327 (LV 6), 159-350, 163-317 (LV 3), 167-317 (LV 2), 168-326 (LV 1), 170-337, 177-341, 182-336, and 244-440 from our raw scanning FP interferograms. The identified proplyds have a conspicuous appearance: they are detected as bright, point-like nebulosities appearing only in some velocity maps. In order to improve the detection of proplyds from

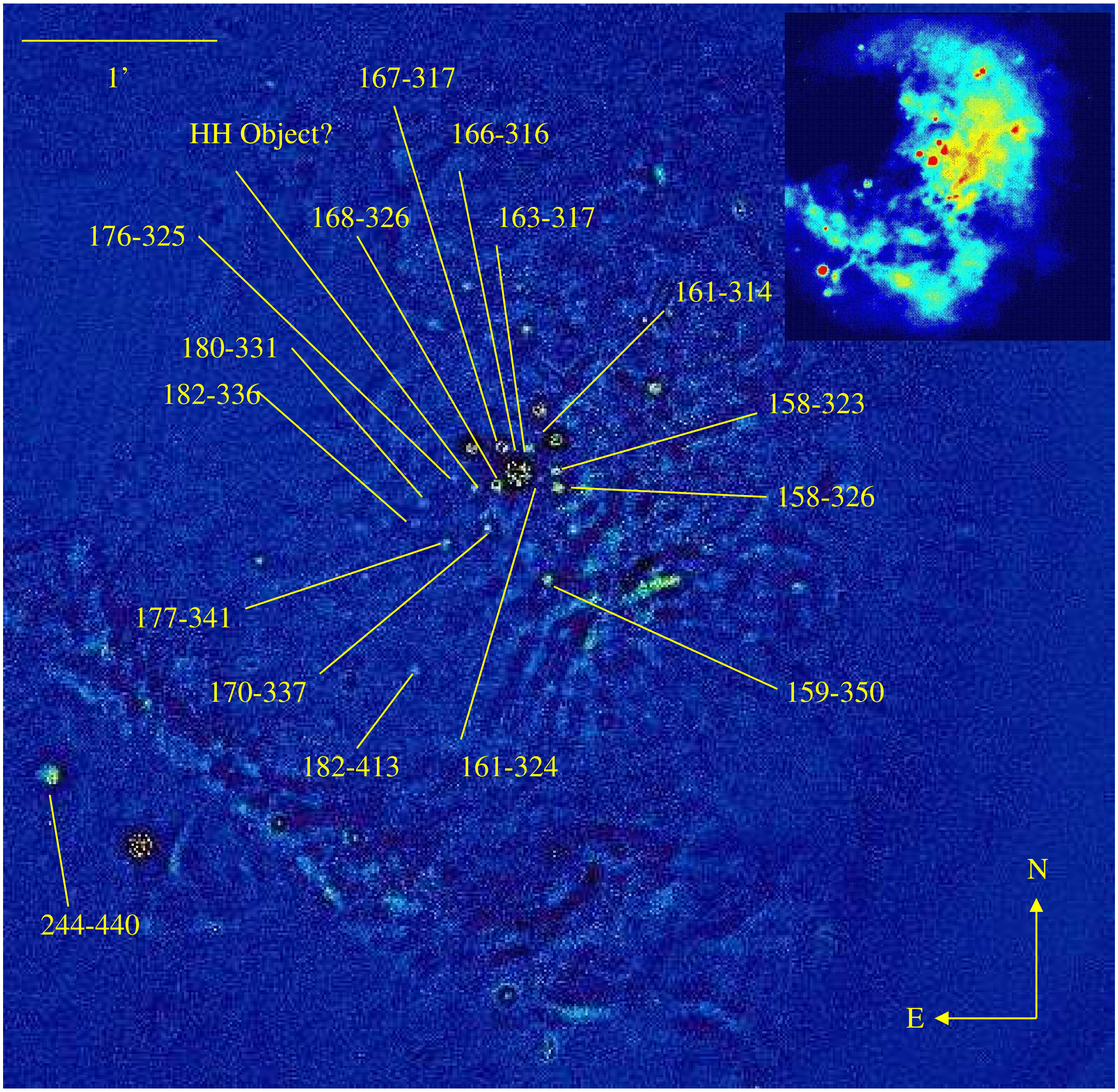

Fig. 1. Unsharp-masked Hα velocity map at heliocentric velocity of $-127\,\mathrm{km\,s^{-1}}$. The original image published by Rosado et al. (2001, 2002) is shown in the insert. The identified proplyds are marked.

our velocity maps we applied an "unsharp-masking" process (Malin 1978) so as to isolate the small diameter emission structures from the bright diffuse H II region (as will be described below). This technique is also useful for detecting extended features embedded in bright emission regions (e.g., Moreno-Corral, de la Fuente, & Gutiérrez 1998).

Figure 1 shows the FP velocity map at $V_{\rm hel} = -127\,\mathrm{km\,s^{-1}}$ shown in Rosado et al. (2002) that results after applying the unsharp-masking process. In this map we have marked the position of the identified proplyds; as seen in this figure, they are quite conspicuous. The unsharp-masking process was carried out in the following way: first, we performed a spatial Gaussian smoothing (with $\sigma = 3$ pixels or $1.77''$) of small diameter features (such as the proplyds and thin filaments). Then, we subtracted the smoothed velocity maps from the original velocity maps. The result is that the small diameter features stand out, whereas the diffuse, extended emission (such as the foreground H II region) is subtracted. In that way we were able to identify the proplyds reported in O'Dell et al. (1998). Indeed, this process improves the detection of proplyds; the proplyds 161-314, 161-324 (LV 4), 166-316, 176-325, 180-331, and 197-427 became noticeable only after applying the unsharp-masking process, while the proplyds already detected in the raw data cubes were more easily distinguished.

3.2. *Proplyd Radial Velocity Profiles*

The extraction of proplyd radial velocity profiles from our FP data is not as straightforward as one could wish, due to the severe contamination from the bright H II region. However, we can use our knowledge of the kinematics of the H II region and the proplyds to obtain the velocity profiles subtracted from the H II region. Indeed, the H II region emits at low redshifted velocities (from +5 to +20 km s^{-1} according to Meaburn (1988) and Rosado et al. (2001), amongst others) while, as discussed in the Introduction, some of the proplyds (or some regions thereof) seem to be characterized by high redshifted velocity features. Taking advantage of this, we proceeded as follows in order to subtract the intense but variable (in position and velocity) H II region:

- First, we constructed from our FP data an integrated radial velocity profile of the central 5′ of the Orion Nebula. This gives us the intensity as a function of the velocity: $I(v)$.
- We also constructed a "monochromatic image" of the Orion Nebula by collapsing the different continuum-subtracted FP velocity maps in one single image.
- We constructed an "H II region velocity cube" by multiplying, for each velocity value v, the monochromatic image by $I(v)$ obtained from the first step. This generates a velocity cube as the series of images that would be expected if there were only the H II region.
- Finally, we subtracted the "H II region velocity cube" from the original velocity cube, one velocity at a time. The resulting velocity cube will have the H II region subtracted, with only the contribution of the high velocity features remaining.

This procedure has certain limitations: (1) the integrated H II region velocity profile, $I(v)$, is slightly broader than a velocity profile extracted only from an individual pixel; (2) the high-velocity features make a contribution to the integrated H II region velocity profile, making the average velocity slightly higher. This second limitation is not so serious because the high-velocity features are rare and most of them are blueshifted. At most, this would imply an oversubtraction of the high-velocity features. Indeed, after extracting the proplyd radial velocity profiles using this H II region subtraction technique, we noted that some blueshifted features, visible in the non-subtracted velocity profiles, were eliminated. Thus, this procedure is excellent for revealing redshifted velocities, but is not so good for blueshifted velocities.

Following this procedure we were able to identify 14 proplyds (and some other high velocity objects) in different velocity maps. Figure 2 shows a close-up of the H II region-subtracted velocity map at $V_{\rm hel} = +119$ km s^{-1}, where most of the proplyds are identified as point-like sources (other proplyds were better identified in the map at $V_{\rm hel} = +62$ km s^{-1}, not shown). From this figure, we note that some of the proplyds revealed after the unsharp-masking procedure are not visible in the subtracted H II region velocity maps. This could be due to the oversubtraction effect mentioned above. This is the case of the proplyds: 161-314, 166-316, and 197-427. Consequently, their velocity profiles are not analyzed in this work. In the case of the proplyd 244-440, although it is well detected in the rough FP velocity maps, we were not able to adequately subtract the H II region. We do not analyze its velocity profile in this work either. On the contrary, some other proplyds and high-velocity features are conspicuous in this map; these are marked in Fig. 2.

After extracting the radial velocity profiles at the proplyd positions we find that most of them show high-velocity wings as already found by Meaburn and collaborators. These velocity profiles were extracted from boxes of 2 pixels per side, centered at the proplyd position.

Figure 3 shows the proplyds' Hα radial velocity profiles obtained in this way (i.e., with the H II region subtracted). It is illustrative to analyze in more detail the velocity profile of the proplyd 167-317 (LV 2) whose H II region-subtracted [O III] velocity profile has been already published in Meaburn et al. (1993). We can see that we find roughly the same velocity profile as the one reported in Meaburn et al. (1993), Figure 5.

In general, the velocity profiles shown in Fig. 3 present some common features: a relatively narrow peak and a high-velocity wing. For some proplyds, the wing is well separated in velocities from the narrow peak; for some other proplyds, the wing has a wide range of velocities and joins the main velocity

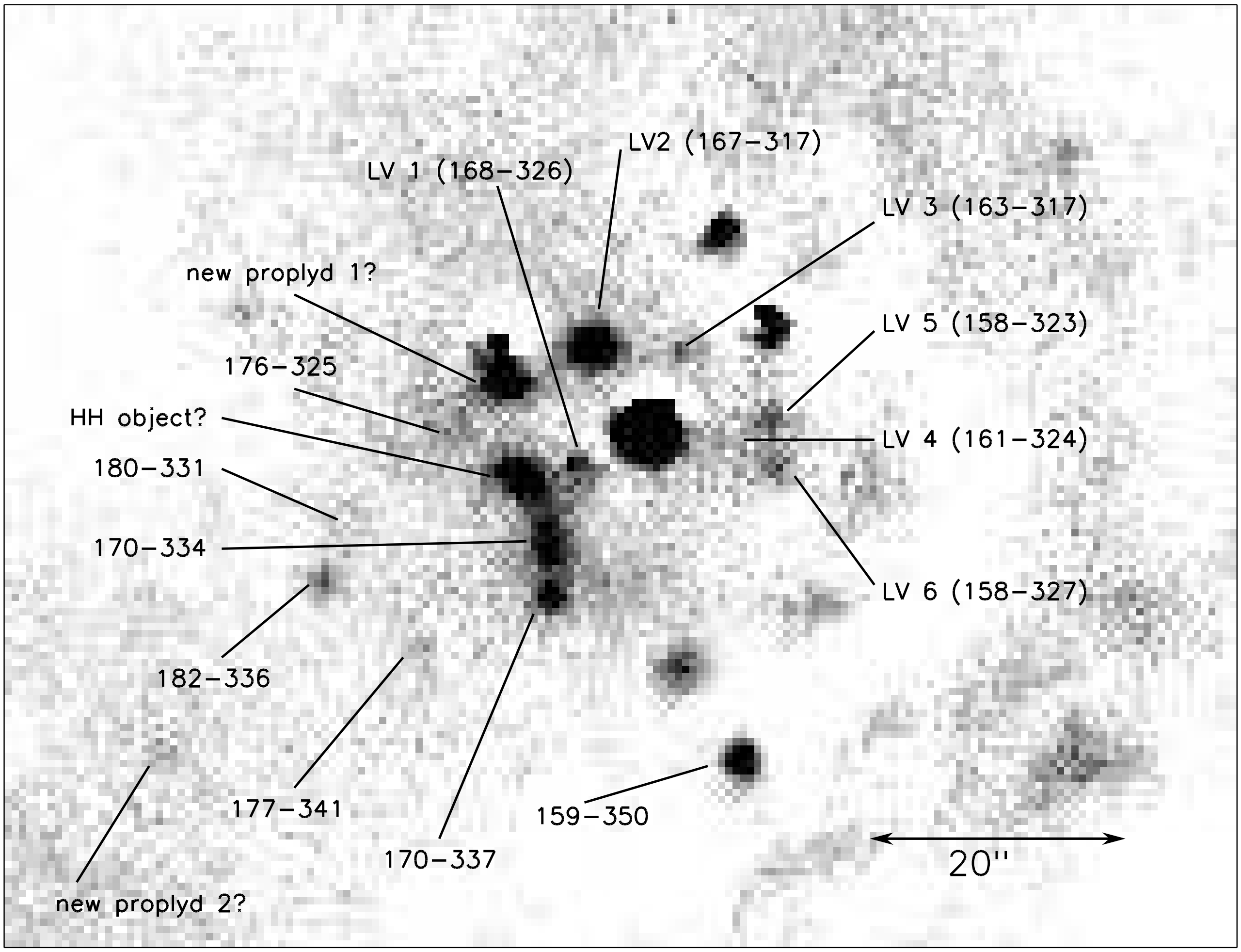

Fig. 2. H II-region-subtracted Hα velocity map at heliocentric velocity = $+119\,\mathrm{km\,s^{-1}}$. The identified proplyds are marked. The identification of 170-334 has been adopted from Fig. 3 of Bally et al. (1998a).

component. However, it is possible that noise magnifies these differences.

In order to quantify and compare the kinematic features mentioned above, in Table 1 we list the main kinematic information derived from the extracted profiles of proplyds. Additionally, we also list the kinematic information derived from already published velocity profiles of some of the proplyds. The main kinematic information quoted is: the peak velocity, the FWHM of the velocity profiles (without any instrumental or thermal broadening correction), the velocity width at $0.05 I_{\mathrm{peak}}$ that we call FWZI, and whether or not a high redshifted wing is detected, quoting its heliocentric velocity, if detected. The FWHM listed here correspond to the main peak, given that the high velocity wing is much fainter.

As seen from Table 1, the values of the quantities we derive from the FP velocity profiles agree quite well with the kinematic information we can derive from other work except in the case of the proplyd 170-337, also reported by Henney & O'Dell (1999). In this case, we detect a high velocity wing not seen in Henney & O'Dell's velocity profiles. It is possible that this difference could be due to the better spatial resolution of Henney & O'Dell (1999) that allows them to extract the velocity profile of only the cusp of the proplyd.

From Table 1 we see that the detected proplyds have peak velocities redshifted relative to the systemic velocity of the Orion Nebula. The FWHM varies between 35 and $60\,\mathrm{km\,s^{-1}}$; most of them show high redshifted wings with heliocentric velocities of up to $+150\,\mathrm{km\,s^{-1}}$. No blueshifted features were detected.

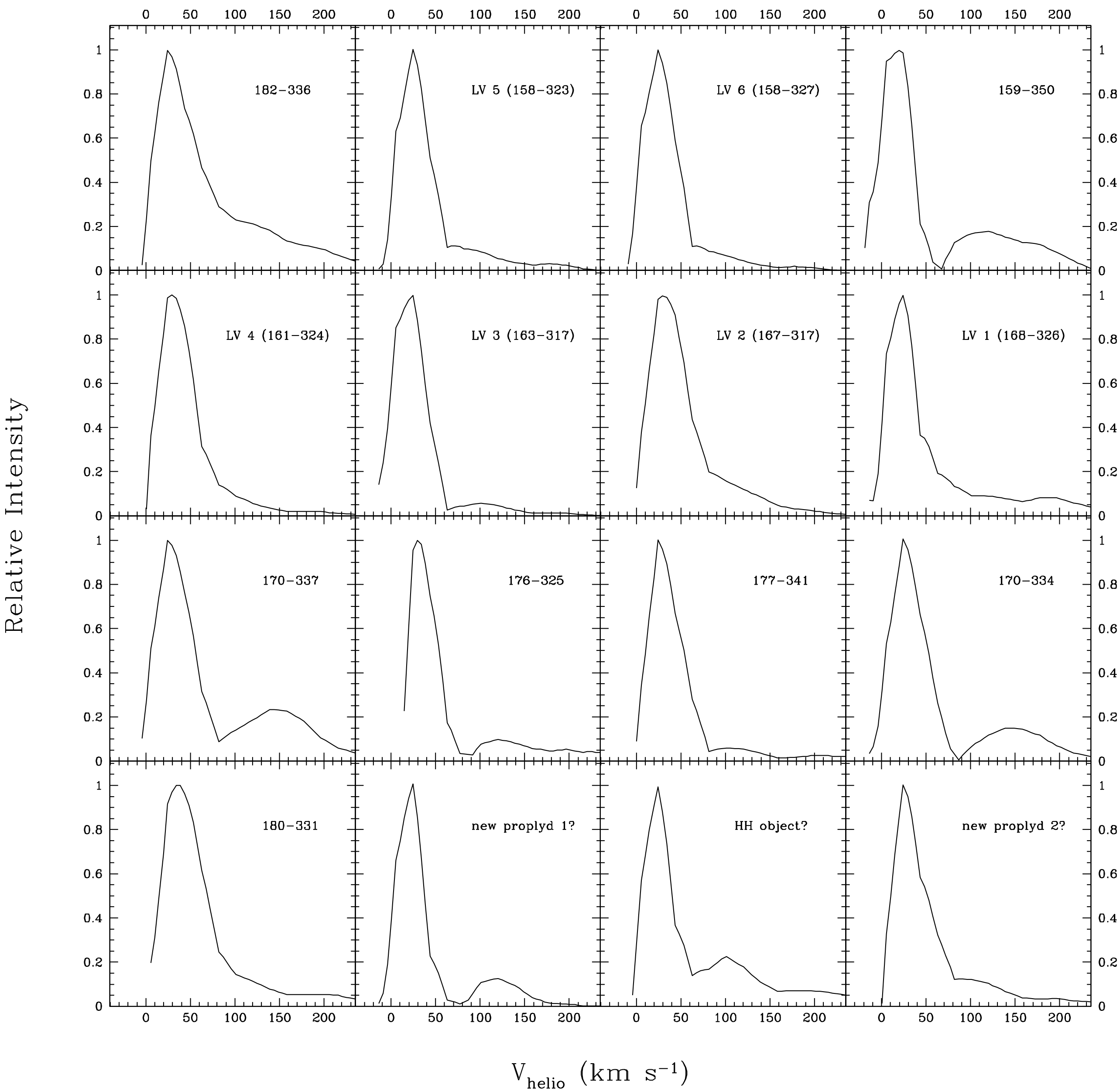

Fig. 3. Radial velocity profiles of the detected proplyds 182-336, 158-323 (LV 5), 158-327 (LV 6), 159-350, 161-314 (LV 4), 163-317 (LV 3), 163-317 (LV 2), 168-326 (LV 1), 170-334, 170-337, 176-325, 177-341, and 180-331. The radial velocity profiles of three proplyd or HH candidates are also displayed (see the text).

3.3. *High Velocity Features Associated with Proplyd Candidates and a New HH Object?*

In Fig. 2 one can see two additional highly red-shifted features already noted by Meaburn et al. (1993) and Massey & Meaburn (1995): a point-like emission feature near the star θ^1 Orionis D that we call "new proplyd 1?" and an extended high-speed loop, also seen in *HST* images as an arc, that we call "HH object?". We also mark the position of another feature (better seen in the velocity map at $V_{\rm hel} = +62\,{\rm km\,s^{-1}}$ as a point-like object) that we call "new proplyd 2?". In Fig. 3, we show the velocity profiles (subtracted from the H II region) of those features, and in Table 1 we also list the kinematic information of these high velocity features derived from the velocity profiles.

The "new proplyd 1?" is seen as point-like and very close to θ^1 Orionis D. Its velocity profile is similar to the velocity profiles of other proplyds and,

TABLE 1

VELOCITY INFORMATION OF THE IDENTIFED PROPLYDS (THIS WORK AND PREVIOUS WORKS)

Proplyd Name[a]	$V_{\rm peak}$[b]	$V_{\rm peak}$	FWHM[b]	FWHM	FWZI[c]	FWZI	$V_{\rm wing}$[d]	$V_{\rm wing}$
158-323 (LV 5)	+25	···	40	···	130	···	+90	+150[e]
158-327 (LV 6)	+25	···	45	···	120	···	+70	···
159-350	+20	···	40	···	240	···	+120	···
161-324 (LV 4)	+30	···	48	···	125	···	+90	···
163-317 (LV 3)	+25	···	44	···	135	···	+100	+76[e]
167-317 (LV 2)	+30	+38[e]	50	60[e]	160	180[e]	+110	+150[e]
168-326 (LV 1)	+24	···	40	···	230	···	+80	+160[e]
170-334	+25	···	48	···	220	−100 to +80[g]	+150	···
170-337	+25	+20[f]	50	50[f]	240	80[f]	+150	···
176-325	+30	···	36	···	195	···	+120	···
177-341	+25	+25[f]	35	45[f]	80	75[f]	No	···
180-331	+38	···	55	···	150	···	+80	···
182-336	+30	···	60	···	230	···	+120	···
new proplyd 1?[h]	+25	···	36	···	165	···	+120	+107[h]
HH object?[i]	+24	···	36	···	240	···	+100	+125(SW)[g] +90(NE)[g]
new proplyd 2?[j]	+25	···	45	···	150	···	+100	···

[a]According to the notation of O'Dell & Wen (1994) and, within parenthesis, Laques & Vidal (1979).

[b]Heliocentric velocity and observed FWHM (not corrected from instrumental effects) of the main peak obtained in this work (in km s^{-1}).

[c]Width of the radial velocity profile at 0.05 $I_{\rm peak}$ (in km s^{-1}) obtained in this work.

[d]Heliocentric radial velocity of redshifted wing (in km s^{-1}) obtained in this work.

[e]From Meaburn et al. (1993), in km s^{-1}. [f]From Henney & O'Dell (1999), in km s^{-1}. [g]From Massey & Meaburn (1995), in km s^{-1}.

[h]Emission feature near θ^1 Orionis D. First reported in Meaburn et al. (1993).

[i]Near LV 1. Appearing in *HST* images as an arc. Extended high-speed loop reported in Meaburn et al. (1993) and Massey & Meaburn (1995).

[j]Point-like in *HST* images. In Fig. 2, to the SW of 82-336.

consequently, we think that this feature is a proplyd not reported as such so far.

The "HH object?" is seen in Fig. 2 as a bow-shaped nebula to the southeast of the proplyd 168-326. First reported by Meaburn et al. (1993) and Massey & Meaburn (1995), it has also been noted by O'Dell et al. (1997) in their [O III] FP red contours. These authors find that the nebulosity is redshifted by about +100 km s^{-1} relative to the H II region velocity, in agreement with the values listed in Table 1. Its bow-shaped morphology was revealed in the *HST* image at [O III] shown in Bally et al. (1998a). These authors suggested that this nebula could be an HH object. However, it is interesting to note that this feature shows only redshifted velocities with respect to the Orion Nebula, while most of the HH objects studied in Rosado et al. (2001) presented blueshifted velocities.

Finally, the other high velocity feature, "new proplyd 2?", shows a velocity profile similar to the other proplyds. Both its appearance and its velocity profile suggest that it could be another proplyd.

4. DISCUSSION

As mentioned above, Table 1 lists the peak velocities of the proplyds obtained from our FP velocity profiles, with the intense emission of the H II region subtracted. As one can see from this table, all the proplyd peak velocities are redshifted relative to the H II region, indicating that all the proplyds studied in this work are located in the same gaseous sheet behind the H II region. However, given that the subtracted H II region moves with velocities close to the proplyds' peak velocities, the proplyds' systemic velocities cannot be very accurate. On the other hand, Table 1 reports the proplyd velocity widths uncorrected from the instrumental and thermal widths. The velocity widths have values between 35 and 60 km s^{-1}, similar to those presented by Meaburn et al. (1993), Massey & Meaburn (1995), and Henney & O'Dell (1999).

For further discussion of our results it is necessary to bear in mind the basic aspects of proplyd models. As mentioned in the Introduction, these models propose that proplyds are formed and detected due to the photoevaporation of the protoplanetary disk by the intense UV radiation of an external star (in this case θ^1 Orionis C, sometimes in combination with θ^2 Orionis A). Different regions of the proplyd give rise to different kinematic features, as discussed in Henney et al. (2002) for the case of LV 2. For this object, high spatial resolution spectroscopy allowed these authors to get velocity profiles of different regions within the proplyd. The proplyd head or cusp can be identified with the portion of the velocity profile between 0 and +60 km s^{-1} (i.e., the main peak). The high velocity wings between +100 to +150 km s^{-1} are indications of the presence of microjets. On the other hand, the LV 2 emission at intermediate velocities (between +60 to +100 km s^{-1}) was found to be of uncertain origin by these authors. Henney et al. (2002) suggested that this emission might be associated with the microjet, or else with a dust-scattered echo.

In the case of our observations, the lower spatial resolution would imply that the proplyd velocity profiles have contributions from different emitting zones of the proplyd that have different kinematics. If we assume that other proplyds could have the same emitting regions, the velocity profiles presented in Fig. 3 show that most of the proplyds studied here seem to have microjets; they are in fact, monopolar microjets since no blueshifted counterpart is detected for any of them. The nondetection of counterjets is understood because the counterjets tend to be much fainter than the redshifted microjets, and they are difficult to detect against the bright nebular emission (Bally et al. 2000). However, the large proportion of proplyds presenting microjet features puzzles us. Indeed, Bally et al. (2000) analyzed Orion's *HST* images and found about 24 proplyds with detected microjets. Only three of the reported microjets from their list coincide with the proplyds studied in this work. It is possible, however, that the jet dimensions are so small that even the *HST* could not resolve some of them. Thus, our results suggest that microjets are more common in proplyds.

With regard to the cusp or head, proplyd models assume that the protoplanetary disk is surrounded by a neutral envelope probably formed by a slow photodissociated wind from the disk. It is also assumed that an ionization front, IF, forms in this envelope and that the newly ionized gas flows away from the proplyd with an initial velocity v_0. Pressure gradients in the ionized gas accelerate the flow away from the IF. The amount of acceleration depends on the type of the IF, being highest when the flow leaving the IF surface is sonic (D-critical IF). The density in the ionized photoevaporated flow is highest at the point on the IF closest to the ionizing star, n_0, and decreases towards the sides. Assuming the flow to be isothermal, and r_0 being the radius of the IF to the point of maximum density, the photoevaporated flow initial velocity, v_0, is related to the disk's photoevaporation mass-loss rate via the relation:

$$\dot{M} = 4\pi r_0^2 v_0 n_0 m_{\rm i}$$

where $m_{\rm i} = 1.35\, m_{\rm H}$, or:

$$\frac{\dot{M}}{10^{-7}\, M_\odot\, {\rm yr}^{-1}} = 0.44 \left(\frac{r_0}{10^{15}\,{\rm cm}}\right)^2 \left(\frac{v_0}{{\rm km\,s}^{-1}}\right) \left(\frac{n_0}{{\rm cm}^{-3}}\right),$$

and the lifetime, τ, of the protoplanetary disk is given by (Johnstone et al. 1998; Henney & O'Dell 1999)

$$\tau \sim M_{\rm disk}/\dot{M}.$$

Thus, the radial velocity profiles of proplyds allow us to constrain the photoevaporated flow velocity. This quantity gives us an estimate of the mass-loss rates of the protoplanetary disks and of the lifetime of those disks.

The quantities n_0 and r_0 are obtained from the fitting of surface brightness profiles of proplyds obtained with the *HST* (Johnstone et al. 1998). In regard to the quantity v_0, the velocity of the recently ionized gas before acceleration, there is some evidence that it is traced by the [O I] (λ6300 Å) emission line, because this line seems to be associated with the flow of neutral gas. Indeed, while the proplyds' protoplanetary disks are seen in absorption in Hα, [N II], and [O III], they are seen in emission at [O I] (Johnstone et al. 1998), indicating that the

TABLE 2

INTRINSIC FWHM, MASS-LOSS RATES, DISK DESTRUCTION TIMES AND PARAMETERS OF THE IDENTIFED PROPLYDS

Proplyd Name[a]	FWHM[i]	r_0[b]	n_0[b]	$M_{\rm disk}$[c]	$\dot{M}$ calculated[h]	$\dot{M}$ others[h]	τ[g]
158-327	14	1.66	0.78	0.064	6.6	6.34[c]	0.97
161-324	22	0.35	6.21	0.009	3.7	0.86[c]	0.24
163-317	10	0.50	4.66	0.021	2.6	2.13[c], 3.5[d]	0.81
167-317	26	0.79	3.86	0.026	13.8	2.64[c], 6.6[d], 8[f]	0.17
170-334	22	0.8[j]	3.0[j]	...	(9.3)	...	...
170-337	26	1.17	1.31	0.042	1.03	3.18[c], 8[e]	0.41
176-325	0.69	1.59	0.032	4.33	0.80[c]	0.73902	
180-331	35	1.22	0.73	0.018	8.4	1.78[c]	0.21
182-336	42	0.8[j]	3.0[j]	...	(18)	...	...
new proplyd 2?	14	0.8[j]	3.0[j]	...	(5.9)	...	...

[a] According to the notation of O'Dell & Wen (1994).

[b] From Henney & Arthur (1998); r_0 in 10^{15} cm and n_0 in 10^6 cm^{-3}.

[c] From Johnstone, Hollenbach & Bally (1998); in $M_\odot$. [d] From Churchwell et al. (1987).

[e] From Henney & O'Dell (1999). [f] From Henney et al. (2002). [g] In 10^5 yr.

[h] In $10^{-7}\,M_\odot\,{\rm yr}^{-1}$; in parenthesis, values calculated from mean values of r_0 and n_0.

[i] Proplyd's FWHM (in km s^{-2}) corrected from instrumental and thermal broadennings. In order to calculate the mass-loss we take $v_0 = 0.5$FWHM(corrected).

[j] Mean values from Henney & Arthur (1998); r_0 in 10^{15} cm and n_0 in 10^6 cm^{-3}.

[O I] emission is tracing the very beginning of the photoevaporated flow before its acceleration. The other ions trace the flow when it is accelerated to some degree. Furthermore, from the velocity profiles of four proplyds at several emission lines presented in Henney & O'Dell (1999) one can see that the velocity widths of the [O I] emission line are, in the four cases, of about 13 km s^{-1}, while the velocity widths of the other emission lines are much broader (up to 40 km s^{-1} for [O III]). In particular, within the errors, the Hα velocity widths are about twice the [O I] widths. Besides, the broadening of the velocity widths increases roughly with the ionization potential of the ion responsible for the emission line. Thus, [O I] velocity widths seem to give directly the velocity of the recently ionized gas before acceleration, v_0, but the widths of the other emission lines would give us an order of magnitude estimate. It should be quite valuable to obtain FP observations in the [O I] line in order to derive, with better accuracy, the mass-loss rates of each proplyd.

Table 1 lists the Hα velocity widths (FWHM) obtained in this work without any correction for the instrumental function and thermal broadening. In Table 2 we list the intrinsic FWHM of the proplyds corrected for the instrumental and thermal widths. In order to do so, we have assumed that the main peak is approximated by a Gaussian function, and that the instrumental and thermal widths can be subtracted in the following way:

$$\big(\mathrm{FWHM(proplyd)}\big)^2 = \big(\mathrm{FWHM(observed)}\big)^2 - \big(\mathrm{FWHM(instrument)}\big)^2 - \big(\mathrm{FWHM(thermal)}\big)^2,$$

where: FWHM(instrument) = 38 km s^{-1} and FWHM(thermal) = 20 km s^{-1} for a gas at 10^4 K. In Table 2 we have not listed the proplyds for which the intrinsic FWHM is comparable to the instrumental + thermal velocity widths.

An inspection of the values of this quantity for the proplyds listed shows that the velocity widths are either smaller or comparable to the ones reported by Henney & O'Dell (1999), and that the Hα velocity widths do not seem to vary as a function of distance to the external ionizing source. Consequently, we expect that the initial flow velocity is comparable to the one found by these authors, i.e., 13 km s^{-1}. In obtaining the mass-loss rates, we thus take v_0 as half of the value quoted in Table 2 for the Hα proplyds' velocity widths. Table 2 also lists the values of r_0, n_0, and of the disk masses taken from other authors, the mass-loss rates calculated by us and compared with estimates of other authors, and the lifetimes of the protoplanetary disks, τ, calculated from our mass-loss estimates.

Our estimated mass-loss rates are the typical mass-loss rates of these objects. The estimated mass-loss rates do not seem to depend on the distance to the ionizing star; however, since our results give only an order of magnitude estimate, this dependency should be corroborated. The $\dot{M}$ have values between 10^{-6} and $10^{-7}\, M_{\odot}\,\mathrm{yr}^{-1}$ and $\tau \sim 10^4$–10^5 yr. Thus, our kinematic work confirms, with a larger number of objects, the conclusions on timescales for disk destruction of 10^5 yr (Henney & O'Dell 1999) that imply the necessity of revising the models of planet formation when very massive stars are forming, as discussed by Throop et al. (2001).

MR wishes to acknowledge the financial support of DGAPA-UNAM via the grant IN104696. E. de la F. wishes to acknowledge financial support from CONACYT-México grants 124449 and 27550-A. The authors would like to thank J. C. Yustis for computer assistance and Jana Benda for revising the text. It is a great pleasure to thank the referee and Bob O'Dell who suggested the procedure for H II region subtraction of the proplyd velocity profiles, and John Bally and Henry Throop for many informative comments and guidelines.

REFERENCES

Bally, J. 2001, AAS, 198, #18.01
Bally, J., O'Dell, C. R., & McCaughrean, M. J. 2000, AJ, 119, 2919
Bally, J., Sutherland, R. S., Devine, C., & Johnstone, D. 1998a, ApJ, 116, 293
Bally, J., Testi, L., Sargent A., & Carlstrom J. 1998b, AJ, 116, 854
Bertoldi, F. 1989, ApJ, 346, 735
Boss, A. P. 1997, Science, 276, 1836
Churchwell, E., Felli, M., Wood, D. O. S., & Massi, M. 1987, ApJ, 321, 516
Dyson, J. E. 1968, Ap&SS, 1, 388
Garay, G., Moran, J. M., & Reid, M. J. 1987, ApJ, 314, 535
García-Arredondo, F., Henney, W. J., & Arthur, S. J. 2001, ApJ, 561, 830
Henney, W. J., & Arthur, S. J. 1998, AJ, 116, 322
Henney, W. J., Meaburn, J., Raga, A. C., & Massey, R. 1997, A&A, 324, 656
Henney, W. J., & O'Dell, C. R. 1999, AJ, 118, 2368
Henney, W. J., O'Dell, C. R., Meaburn, J., Garrington, S. T., & López, J. A. 2002, ApJ, 566, 315
Johnstone, D., Hollenbach, D., & Bally, J. 1998, ApJ, 499, 758
Laques, P., & Vidal, J. L. 1979, A&A, 73, 97
Le Coarer, E., Rosado, M., Georgelin, Y., Viale, A., & Goldes, G. 1993, A&A, 280, 365
Malin, D. F. 1978, Nature, 276, 591
Massey, R. M., & Meaburn, J. 1993, MNRAS, 262, L48
________. 1995, MNRAS, 273, 615
Meaburn, J. 1988, MNRAS, 233, 791
Meaburn, J., Massey, R. M., Raga, A. C., & Clayton, C. A. 1993, MNRAS, 260, 625
Moreno-Corral, M. A., de la Fuente, E., & Gutiérrez, F. 1998, RevMexAA, 34, 117
O'Dell, C. R. 1998, AJ, 115, 263
O'Dell, C. R., Hartigan P., Bally, J., & Morse, J. A. 1997, AJ, 114, 2016
O'Dell, C. R., & Wen, Z. 1994, ApJ, 436, 194
O'Dell, C. R., Wen, Z., & Hu, X. 1993, ApJ, 410, 696
Rosado, M., et al. 1995, RevMexAA(SC) 3, The Fifth Mexico-Texas Conference on Astrophysics: Gaseous Nebulae and Star Formation, eds. M. Peña & S. Kurtz (México, D. F.: Inst. Astron. UNAM), 263
Rosado, M., de la Fuente, E., Arias, L., Raga, A. C., & Le Coarer, E. 2001, AJ, 122, 1928
Rosado, M., de la Fuente, Arias, L., Raga, A. C., & Le Coarer, E. 2002, RevMexAA(SC) 13, Emission Line From Jet Flows, eds. W. J. Henney, W. Steffen, L. Binette, & A. Raga (México, D. F.: Inst. Astron. UNAM), 91
Ruden, S. P. 1999, in The Origin of Stars and Planetary Systems, eds. C. Lada & D. Kylafis (Dordrecht: Nato Science Series, Kluwer Academic Publishers), 643
Sargent, A. I. 1996, in Lecture Notes in Physics 465, Disks and Outflows around Young Stars, ed. S. V. W. Beckwith (Berlin: Springer), 1
Storzer, H., & Hollenbach, D. 1999, ApJ, 515, 669
Throop, H. B., Bally, J., Esposito, W. L., & McCaughrean, M. J. 2001, Science, 292

Patricia Ambrocio-Cruz, Lorena Arias, and Margarita Rosado: Instituto de Astronomía, UNAM, Apartado Postal 70-264, 04510 México, D. F., México (margarit@astroscu.unam.mx).
Eduardo de la Fuente: Instituto de Astronomía y Meteorología, Departamento de Física, CUCEI, Universidad de Guadalajara, Av. Vallarta No. 2602, Colonia Arcos de Vallarta, 44130 Guadalajara, Jalisco, México (edfuente@astroscu.unam.mx).